Spectral bifurcations in dispersive wave turbulence

David Cai,* Andrew J. Majda, David W. McLaughlin, and Esteban G. Tabak

Courant Institute of Mathematical Sciences, New York University, New York, NY 10012

Contributed by Andrew J. Majda, September 30, 1999

Dispersive wave turbulence is studied numerically for a class of one-dimensional nonlinear wave equations. Both deterministic and random (white noise in time) forcings are studied. Four distinct stable spectra are observed—the direct and inverse cascades of weak turbulence (WT) theory, thermal equilibrium, and a fourth spectrum (MMT; Majda, McLaughlin, Tabak). Each spectrum can describe long-time behavior, and each can be only metastable (with quite diverse lifetimes)—depending on details of nonlinearity, forcing, and dissipation. Cases of a long-lived MMT transient state decaying to a state with WT spectra, *and vice-versa*, are displayed. In the case of freely decaying turbulence, without forcing, both cascades of weak turbulence are observed. These WT states constitute the clearest and most striking numerical observations of WT spectra to date—over four decades of energy, and three decades of spatial, scales. Numerical experiments that study details of the composition, coexistence, and transition between spectra are then discussed, including: (*i*) for deterministic forcing, sharp distinctions between focusing and defocusing nonlinearities, including the role of long wavelength instabilities, localized coherent structures, and chaotic behavior; (*ii*) the role of energy growth in time to monitor the selection of MMT or WT spectra; (*iii*) a second manifestation of the MMT spectrum as it describes a self-similar evolution of the wave, *without temporal averaging*; (*iv*) coherent structures and the evolution of the direct and inverse cascades; and (*v*) nonlocality (in *k*-space) in the transferral process.

1. Introduction

Waves in nature, such as waves on the surface of the sea or turbulent waves in the atmosphere, are phenomena so complex that their description must be statistical. Currently, statistical descriptions of nonlinear waves are being proposed and developed that would play the role for waves that statistical physics plays in mechanics—namely, to provide an efficient description of macroscopically observable phenomena through statistical averages. Goals of such theories include (*i*) the prediction of wave spectra (the average energy density of the waves as a function of their wavelength), which are relatively easy to observe in nature; and (*ii*) the parametrization of small scales for large scale simulations. It is a difficult problem to assess the accuracy and validity of these statistical wave theories, primarily because of mathematical and computational difficulties in the nonlinear partial differential equations that provide the fundamental description of the waves' evolution.

In this paper, we study a class of nonlinear wave equations that was introduced in ref. 1 as a simple model for which the validity of theories of dispersive wave turbulence could be precisely checked numerically. Here, further numerical experiments are performed on this model—with the forcing usually restricted to long wave lengths and with dissipation restricted to short waves (direct cascade) and very long waves (inverse cascade). At intermediate spatial scales there is no forcing or dissipation, and the system is conservative in this "inertial range." Both stochastic (white-noise) and deterministic (constant in time) forcings are investigated.

We find four distinct wave spectra within this single model system—the (*i*) direct and (*ii*) inverse cascades of weak turbulence (WT) theory (2), (*iii*) thermodynamic equilibrium, and (*iv*) the new spectra (MMT; Majda, McLaughlin, Tabak) reported in ref. 1. Which spectrum occurs depends on details of nonlinearity, forcing, and dissipation. Each of these four spectra can describe the long-time behavior of the system, and each can be only metastable (with quite diverse lifetimes)—depending again on details of nonlinearity, forcing, and dissipation. For example, we observe a metastable WT spectrum decaying to the MMT spectrum, and conversely, in other regimes we observe an MMT spectrum decaying to a WT spectrum.

In the case of freely decaying turbulence (after the forcing has been turned off), we find that WT is the robust slowly decaying state. In fact, in this freely decaying setting, we observe both the direct and inverse cascades of WT theory—extremely cleanly for the direct cascade, over four decades of energy scales and three decades of spatial scales. These new numerical experiments of freely decaying states present the most striking observations of WT spectra to date, and they should cause reevaluation of some current ideas about the mechanisms behind weak turbulence.

In the case of deterministic forcing, we observe a sharp distinction in behavior between focusing and defocusing nonlinearities. In the focusing case, long-wave instabilities convert the long-wave forcing into an effective stochastic forcing, which then causes a steady transfer of excitations to the dissipation scale and sets up the steady wave spectra—whose front [in momentum (k) space] is described by the MMT spectrum, and the interior (or wake in k-space) described by the WT direct cascade. This initial conversion of steady forcing to an effective stochastic forcing is accomplished through spatially localized solitary waves and the associated focusing instabilities. The defocusing nonlinearity is far less effective in converting the deterministic forcing to an effective stochastic force. Here the coherent states are extended radiation states, which are stable and not efficient as an effective random stirring.

Multiple spectra can be present simultaneously, but at different spatial scales. We emphasize the role of coherent structures in energy transfer mechanisms that set up multiple stable spectra. Moreover, we describe experiments that illustrate the very nonlocal k-space nature of the transferral of energy. Taken together, these experiments provide considerable insight into the mechanisms by which nonlinear waves transfer excitations from the spatial scales of the forcing to the dissipation scales, and the role of nonlinear coherent excitations and their turn-over times in these transferral processes.

Over the years, numerical studies of the spectra of turbulent phenomena have proven difficult, contradictory, and inconclusive. We believe that our numerical study, although restricted to an idealized class of one-dimensional model equations (1), has broad implications about the nature of turbulence in general. In most numerical studies of turbulence, computational limitations severely restrict the decades over which spectra can be observed, making such numerical observations difficult to interpret and to rely on. As an example of the difficulties in two-dimensional fluid turbulence, different groups (3–5) in careful studies observe different and distinct spectra in their numerical experiments. Similar studies of turbulence for fluids with rotation which are relevant for atmospheric flows were reported in ref. 6. In each of these studies, the presence of coherent vortices

---

Abbreviations: WT, weak turbulence; MMT, Majda, McLaughlin, Tabak (see ref. 1); SSS, statistically steady state.

*To whom reprint requests should be addressed. E-mail: cai@cims.nyu.edu.

alters the observed spectra. These distinct observations are very reminiscent of the two spectra that we observe in our model with focusing nonlinearity. In our studies, the distinct time scales associated with different coherent excitations (and the comparison of these time scales with natural mixing and turnover times) produces an interpretation of the mechanisms responsible for the different spectra—an interpretation that is likely to extend to more realistic settings of fluid turbulence. In any case, our numerical study indicates that the one-dimensional class of models introduced in ref. 1 permits precise numerical experiments toward the resolution of issues necessarily left ambiguous in the simulations of more realistic models of turbulence in two and three spatial dimensions.

2. Background

Model Nonlinear Wave Equation. A model system was introduced in ref. 1 for the purpose of testing and clarifying the assumptions of the theory of weak-turbulence via four-wave resonances. This model takes the form

$$iq_t = |\partial_x|^\alpha q \pm |\partial_x|^{-\sigma}\left(\left||\partial_x|^{-\sigma}q\right|^2|\partial_x|^{-\sigma}q\right), \qquad [1]$$

or equivalently in "k-space"

$$i\hat{q}_t = \omega(k)\hat{q} \pm \int \frac{\hat{q}(k_1)\hat{q}(k_2)\hat{q}^*(k_3)}{|k_1|^\sigma|k_2|^\sigma|k_3|^\sigma|k|^\sigma}\delta(k_1+k_2-k_3-k)\,dk_1\,dk_2\,dk_3. \qquad [2]$$

This model depends on two real parameters, $\alpha > 0$ and σ. The parameter σ is introduced to control the nonlinearity. For $\sigma = 0$, a standard cubic nonlinearity results. The parameter α controls the dispersion relation $\omega(k) = |k|^\alpha$, which, for $\alpha < 1$, leads to resonance quartets in this model; that is, to nontrivial solutions of

$$k_1 + k_2 = k_3 + k$$
$$\omega(k_1) + \omega(k_2) = \omega(k_3) + \omega(k).$$

The $\pm$ sign is quite important in determining the properties of the nonlinear waves of this model equation, with the $-(+)$ sign representing focusing (defocusing) nonlinearity. The focusing case is the most unstable—with indefinite Hamiltonian, long-wave instabilities, and solitary waves. In contrast, waves in the defocusing case behave more linearly—much as radiation in linear wave equations.

Dispersive Wave Turbulence. The characteristic feature of dispersive wave turbulence is *flux in k-space*; that is, the flow of excitations from long spatial scales to short ones (the *direct cascade*), or from short spatial scales to long ones (the *inverse cascade*). Conceptually, such fluxes could be created by adding forcing and damping terms to the wave Eq. **2**—each of which is restricted to relevant spatial scales, that is, "localized in k-space." For example, a balance between forcing that is restricted to $k \simeq 0$ and damping restricted to $|k| > K_d \gg 0$ could set up a direct cascade. Thus, to provide the flexibility to study both direct and inverse cascades, we add damping terms to Eq. **2** that are restricted to $k \simeq 0$ and to $|k| > K_d$, as well as forces that are localized in k space. Throughout the *inertial ranges*, there is no forcing nor dissipation, and the free Eq. **2** holds. For some of the numerical experiments, this force is white noise in time, and for other experiments, it is deterministic and steady. The dissipation terms are of the form $-i\Gamma_i\hat{q}(k)$, where $\Gamma_1 > 0$ (restricted to $k \simeq 0$), $\Gamma_2 > 0$ (restricted to $|k| > K_d$), with no dissipation elsewhere.

Two Types of Spectra. The spectra of dispersive wave turbulence are described through two point correlation functions,

$$n(k,t) \equiv \langle \hat{q}(k,t)\hat{q}^*(k,t)\rangle, \qquad [3]$$

where in our numerical study $\langle\cdots\rangle$ denotes time average. The general goal of theories of dispersive wave turbulence is to obtain a closed equation for the correlation functions $n(k,t)$.

The classical closure, known as WT theory (2), is summarized in ref. 1, together with its steady state spectra for Eq. **2**:

$$n(k) = c \text{ equipartition of particle number} \qquad [4]$$

$$n(k) = \frac{1}{\omega(k)} \text{ equipartition of energy} \qquad [5]$$

$$n(k) = |k|^{8\sigma/3-1} \text{ direct cascade} \qquad [6]$$

$$n(k) = |k|^{8\sigma/3-1+(\alpha/3)} \text{inverse cascade.} \qquad [7]$$

These statistically steady state (SSS) spectra are time-independent solutions of the kinetic equations of weak turbulence. Their associated fluxes in k-space will have the correct signs for both direct and inverse cascades for only a limited range of the parameters: $\sigma < (3-4\alpha)/8$ or $\sigma > 3/8$. As parameters cross these ranges, WT theory would indicate detectable changes in observed behavior.

In the numerical experiments reported in ref. 1 the spectra predicted by WT theory were not observed. Rather, the observed spectra had exponents different from those predicted by WT theory. Moreover, these observed spectra agreed with the predictions of an alternative closure (MMT) that was heuristically proposed in ref. 1. For Eq. **1** at $\alpha = 1/2$, this spectrum is

$$n(k) = |k|^{2\sigma-5/4} \text{ direct cascade.} \qquad [8]$$

Numerical Algorithm. We simulate the full dynamics of our system by using a pseudospectral method in combination with an integrated factor method (for details, see ref. 1). For the time dynamics, we use a 4th-order adaptive stepsize Runge–Kutta integrator. For most runs, the total number of modes is 2^{13}, and the system size $L \sim 400$. The largest number of modes we use to selectively verify our results is 2^{16}.

In the following, we will describe the details of our numerical experiments. We will use the convention that the unit for the wavenumber k is $2\pi/L$, thus k is labeled by integers.

3. Results

Four Spectra. We begin in a freely decaying setting, in which both the direct and inverse WT cascades are observed. First, we create a sufficiently stirred state that evolves from a smooth initial data under a random forcing at long wavelengths. This state is then used as initial conditions for our weakly decaying studies, for both defocusing and focusing nonlinearities and for various σ and α values. Then, to study freely decaying WT, we set the force at 0 and add damping Γ_1 on large spatial scales $|k| \sim 1$ and Γ_2 on small spatial scales $|k| > K_d$. ($K_d = 2600$ for most experiments.) When $\Gamma_1 \ll \Gamma_2$, the state gradually relaxes to the direct WT cascade. As shown in Fig. 1*b*, this WT spectrum occurs over *four* decades of energy, and *three* decades of spatial scales. Alternatively, when $\Gamma_1 \gg \Gamma_2$, i.e., stronger dissipation on large spatial scales, the state relaxes to the inverse WT cascade, as clearly shown in Fig. 1*c*. Theoretically, the spectrum of WT direct cascade is independent of α, a fact confirmed (not shown) in our freely decaying numerical simulations. We emphasize that throughout these studies of freely decaying turbulence, the states remain nonlinear.

As described in *Two Types of Spectra*, for the theoretical WT spectra to be physically meaningful, the direction of their fluxes in k-space should be consistent with those of the direct and

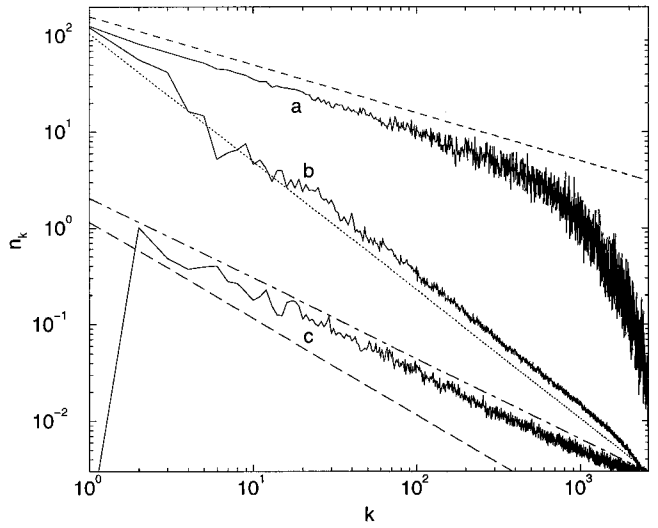

Fig. 1. (*a*) Thermodynamical equilibrium under relaxation dynamics (focusing nonlinearity, $\alpha = 1/2$, $\sigma = 0.25$). The short dashed line has the slope of energy equipartition, $n(k) \sim \omega(k)^{-1}$ (Eq. 3). (*b*) Direct cascade WT spectrum under relaxation dynamics (defocusing nonlinearity, $\alpha = 1/2$, $\sigma = -0.125$). The slope of the dotted line is the prediction of the WT theory for direct cascade. (*c*) Inverse cascade WT spectrum under relaxation dynamics (defocusing nonlinearity, $\alpha = 1/2$, $\sigma = 0$). The slope of the dot-dashed line is the prediction of WT theory for inverse cascade. For comparison, the prediction of WT direct cascade is also shown (dashed line). Note that, for clarity, spectra *b* and *c* have been shifted down by a factor of 10 and 100, respectively.

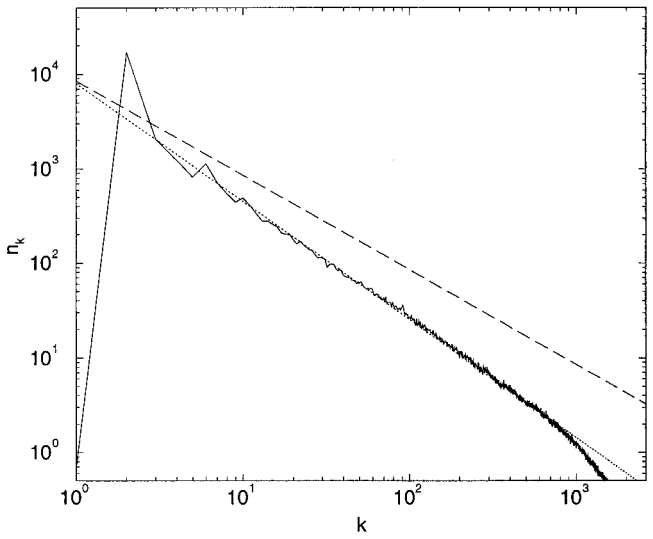

Fig. 2. MMT spectrum of driven-damped dynamics (defocusing nonlinearity with $\alpha = 1/2$, $\sigma = 0$). The system is driven by a random force at $|k| = 2$ and is damped at $|k| = 1$ and $|k| > 2600$. The slope of the dotted line is the prediction of the MMT closure and, for comparison, the dashed line has the direct WT cascade slope.

inverse cascades. For $\alpha = 1/2$, the predicted value for this bifurcation is $\sigma = 1/8$, with one physical regime $\sigma < 1/8$. We have studied this potential bifurcation numerically with relaxation dynamics over the range $-1/4 < \sigma < 1/4$. For $\sigma < 1/8$, our numerical results show (for $\Gamma_2 \gg \Gamma_1$) that the freely decaying states have the WT direct cascade spectra. For $\sigma > 1/8$, the relaxation does not lead to any clear power law for $n(k)$. This transition is not sharp as σ crosses $1/8$.

For focusing nonlinearity, in addition to the two WT spectra described above, there is a *third* spectrum emerging under relaxation dynamics (see Fig. 1*a*)—thermodynamic equilibrium spectrum, i.e., $n(k) \sim \omega(k)^{-1} \sim k^{-1/2}$. Unlike the defocusing case, focusing nonlinearity can destablize long waves when the amplitude of these waves is sufficiently large. This well known "modulational instability" creates spatially localized coherent structures, whose statistical behavior can be captured by a "most probable state description" that predicts these states live in thermodynamic equilibrium. A similar scenario is observed in the case of a driven-damped nonlinear Schrödinger equation, where modulational instability leads to spatiotemporal chaos (7). In this context of non-dissipative Schrödinger equations, a recent equilibrium statistical theory for most probable states successfully predicts the coherent structure as well as energy equipartition (8).

We now turn to a *fourth* spectrum (MMT), which is shown in Fig. 2 for the defocusing nonlinearity. This steady state is achieved by random forcing (Gaussian white noise in time) on low k, with strong damping at high $|k| > K_d$. This experiment demonstrates that, with defocusing nonlinearity, a state with MMT spectrum can be very long-lived.

Having established the existence of four distinct stable spectra, we turn to more detailed descriptions—such as their simultaneous existence, transition between them, and the role of coherent structures in these processes.

Deterministic Forcing. When the system is driven by a steady forcing on low $|k|$ modes, the *defocusing* dynamics has spectrum shown in Fig. 3*a*, which exhibits a statistically steady state with the coexistence of direct WT spectrum on high k modes and a resonance spectrum on low k modes. These Hamiltonian resonances—which are reminiscent of the "pre-Kolmogorov" spectrum observed in the numerical studies of the *kinetic* equation (9)—permeate from low k through intermediate k modes and create a "stochastic layer" on higher k modes. Waves on this stochastic layer in turn pump energy to high k modes and induce sufficient decoherence of those high k modes, resulting in a WT direct cascade. In contrast, for *focusing* nonlinearity with deterministic driving at a moderate amplitude, the motion of long waves becomes chaotic because of modulational instability, which quickly generates a wave turbulence inertial range

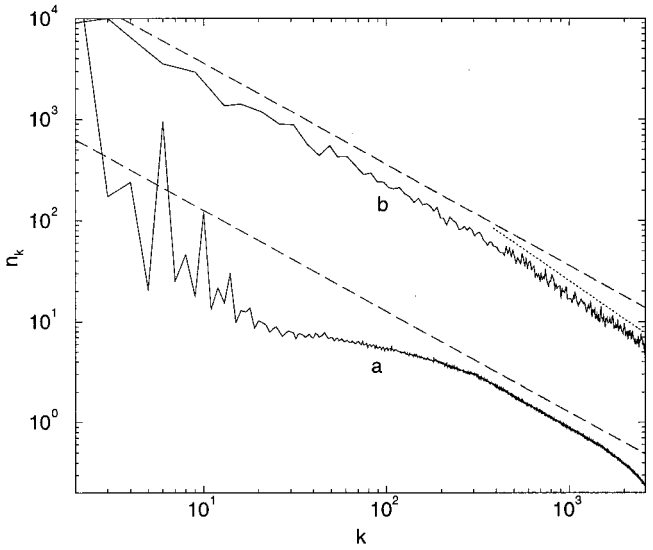

Fig. 3. Steady deterministic force. (*a*) Coexistence of a WT direct cascade with Hamiltonian resonances in an SSS, for the *defocusing* dynamics ($\alpha = 1/2$, $\sigma = 0$), driven by a steady force on $2 \le |k| \le 4$. (*b*) Invasion of WT direct cascade into the MMT transient regime, for the *focusing* nonlinearity ($\alpha = 1/2$, $\sigma = 0$), driven by a steady force on $2 \le |k| \le 3$. The initial data for these cases is smooth, composed of a simple sum of $A_i \mathrm{sech}(A_i(x - x_i))$, $1 \le i \le 3$, the location x_i being arbitrarily chosen. Note that spectrum *b* has been shifted up by a factor of 10^2 for clarity.

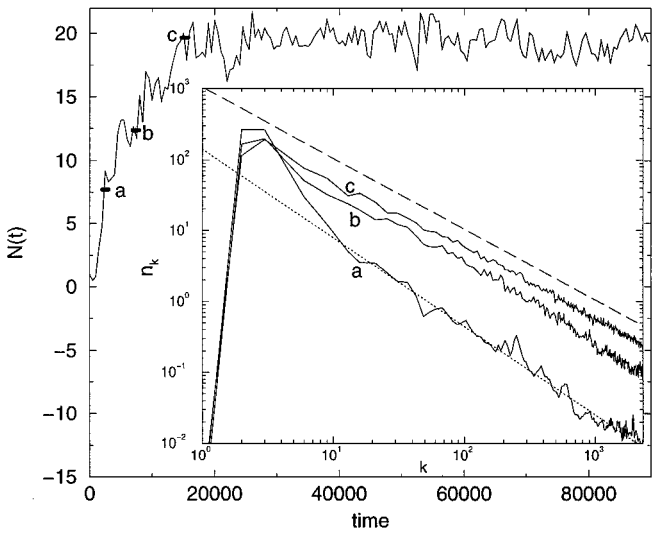

Fig. 4. Temporal growth of L^2 norm [$N(t)$]. *a*, *b*, and *c* correspond to the three spectra in the *Inset*. The location and the length of the line segment indicate the time and the time window used in averages to obtain the corresponding spectrum. (*Inset*) Transition ($a \rightarrow c$) from the MMT regime to the WT direct cascade in the *focusing* dynamics ($\alpha = 1/2$, $\sigma = 0$) driven by a random force on $2 \leq |k| \leq 3$. The slope of the dotted (dashed) line is the prediction of the MMT (WT) closure.

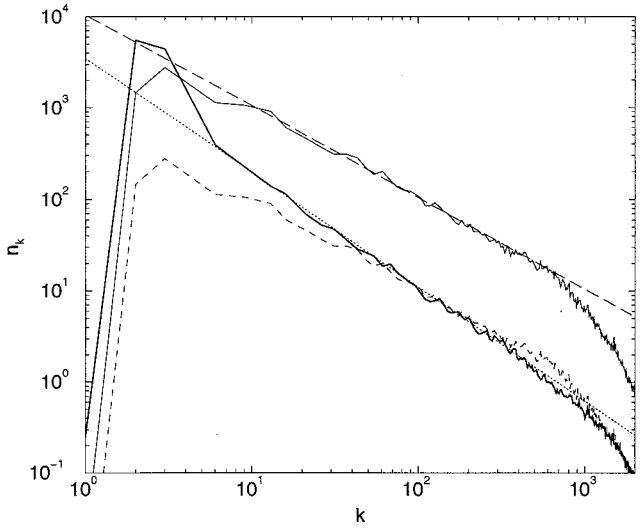

Fig. 5. MMT (thick line) state as the SSS in the *defocusing* dynamics ($\alpha = 1/2$, $\sigma = 0$), driven by a random force, which evolves from a transient WT direct cascade. The WT direct cascade is indicated by the short dashed line and, for clarity, is shifted up by a factor of 10 as indicated by the fine line. The dotted line has the MMT exponent and the dashed line has the WT direct cascade exponent.

starting from very low k modes. In this focusing case, initially the MMT spectrum is observed over the entire initial range. However, it is a transient and the WT direct cascade spectrum gradually invades from low k modes while the range of the MMT spectrum shrinks toward high k modes and eventually disappears, leaving the WT spectrum over the entire inertial range. Fig. 3*b* shows an intermediate stage of this transient, in which both spectra coexist. Next, we will discuss such transitions from the MMT to WT, *and vice versa*.

Transition Between the MMT and WT Spectrum. This transition from the MMT to WT direct cascade spectrum is also observed for focusing nonlinearity under *random* forcing. In the focusing case, we can correlate each stage of expansion of the WT spectrum and contraction of the MMT spectrum with the growth of L^2 norm, as shown in Fig. 4. When driving is large, the growth of norm is fast and the total averaged norm is large in the final steady state. With increasing norm, the nonlinearity increases and the time scale for wave interaction becomes short. A case of relatively strong nonlinearity is shown in the *Inset* of Fig. 4, which depicts three stages of coexistence of the two spectra. Here, the WT direct cascade finally establishes itself as an SSS whose norm fluctuates in time about a constant mean. When the drive becomes weak, the resulting nonlinearity can lead to a very large time scale for nonlinear turn-over and an extremely slow growth of L^2 norm. In this regime, the MMT spectrum can persist for a very long time—for some focusing cases, as long as $\sim 10^5$ time units (not shown). The MMT spectra reported in ref. 1 were in this weakly nonlinear regime.

Now we turn to a case of the *defocusing* nonlinearity, in which (numerically) the MMT spectrum describes statistically steady states. Fig. 5 shows an example in which the defocusing dynamics initially exhibits a WT direct cascade, and eventually becomes the MMT spectrum. This transition from the WT direct cascade to the MMT spectrum provides our strongest numerical evidence that the MMT can describe a stable SSS. (Alternatively, for much weaker damping in high k dissipative range, we note that a WT direct cascade describes the SSS).

Wave Front in *k*-Space. In addition to the interesting interplay between the WT and MMT spectra in the time averaged, statistical sense, we now show that, even without averaging, both of these spectra also appear in k-space wave motion. Fig. 6 depicts the *solution*, $n(k,t) = \hat{q}(k,t)\hat{q}^*(k,t)$, evolving from a smooth initial data (*without* time average) for the *focusing* nonlinearity with steady forcing. Surprisingly, the envelope of the wave fronts in the k-space has a power law form with the MMT exponent, as clearly seen in Fig. 6, while the wake of the wave in the k-space displays the exponent of the WT direct cascade (not shown). Thus, the MMT spectrum can arise in at least two distinct manners: (*i*) the statistical response to driving and damping and (*ii*) the fast dynamics of the wave front propagation in k-space. The latter wave front propagation in k-space can be traced (not shown) to a self-similar formation of localized coherent structures in x-space, and is not observed for *defocusing* nonlinearity.

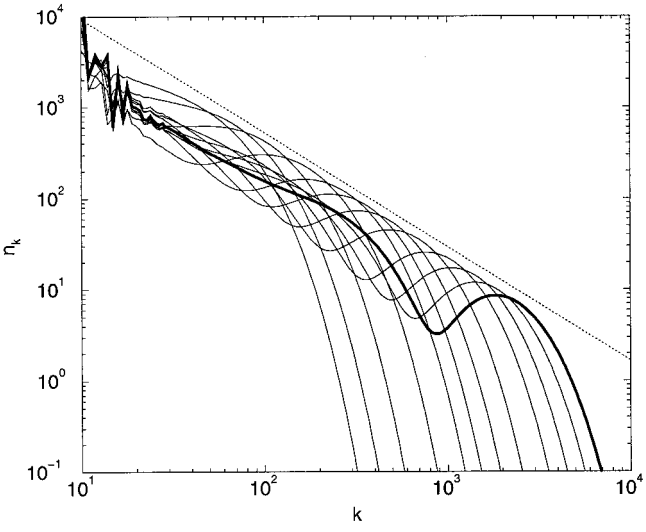

Fig. 6. Wave motion in k-space. *Solutions* for the *focusing* nonlinearity ($\alpha = 1/2$, $\sigma = 0$), driven by a steady force on $1 \leq |k| \leq 2$ evolving from a smooth initial data. Note that *no time average* is used here. Each curve represents $n(k,t) = \hat{q}(k,t)\hat{q}^*(k,t)$ at a different time (not necessarily evenly sampled in time). The large k envelope exhibits the MMT exponent (dotted line).

Coherent Structures and Resonant Waves in Energy Transfer—Coexistence of Equilibrium, Inverse, and Direct Cascades. The next numerical experiment illustrates the cycle of energy transfer in the SSS—a cycle that involves interaction of coherent structures and resonant waves as they form the equilibrium, inverse and direct WT cascades simultaneously. As described above, modulation instability in our focusing dynamics induces spatially coherent "solitonic" excitations at random spatial locations to form a thermal equilibrium bath. The formation of these excitations can actively transfer energy into high k_s via their focusing processes in space, where the wavenumber k_s is determined by the spatial scale of these localized waves. This energy injection process associated with the creation of the localized excitations is a relatively fast process, while the decay of these coherent structures is slow, and gradually transfers energy back from the scale of k_s to low k via the radiation of long waves. The long wave radiation consists of relatively coherent waves, which can participate in wave resonant interactions. Thus, we expect this radiation to form a WT inverse cascade. This is indeed the case. Fig. 7*a* shows an excellent example of the coexistence of a thermodynamical equilibrium state of these coherent structures and the inverse cascade induced by their slow radiation of long coherent waves. For spectrum a, we have $k_s > 1000$. We note that, for k even higher than k_s, the usual WT direct cascade should be expected, since the coherent excitations do not have strong influence on energy transfer at spatial scales much smaller than their coherence length. Fig. 7*b* demonstrates this phenomenon, where we have tuned the dynamics to a regime such that only very few long waves are unstable. These inject energy into $k_s \sim 100$, resulting an inverse cascade for $k < k_s$ and a direct cascade for $k > k_s$. (To help in the interpretation of these equilibrium spectra, we note that, in general, the distribution for the thermodynamical equilibrium is $1/(\omega + \mu)$, where μ is chemical potential. We are able to tune the value of μ in our experiments by controlling the forcing strength. The thermodynamical equilibrium distribution of those unstable long mode $\tilde{k}$ in Fig. 7 corresponds to the limit in which $\mu \gg \omega(\tilde{k})$.) We emphasize that the formation and decay of coherent excitations in thermal equilibrium, together with the resonance wave interaction of the direct and inverse cascades induced by the coherent excitations, form a complete cycle of energy transfer in SSS—in contrast from standard descriptions in plasma turbulence, which only utilize collapse with high k dissipation (10, 11). Finally, we point out that, even when driven extremely strongly, e.g., a value so strong that the total norm is increased by a factor of 10^2 with respected to the cases shown in Fig. 7, the *defocusing* dynamics does not possess this energy transfer cycle simply because it does not have long wave instabilities, and *localized* excitations.

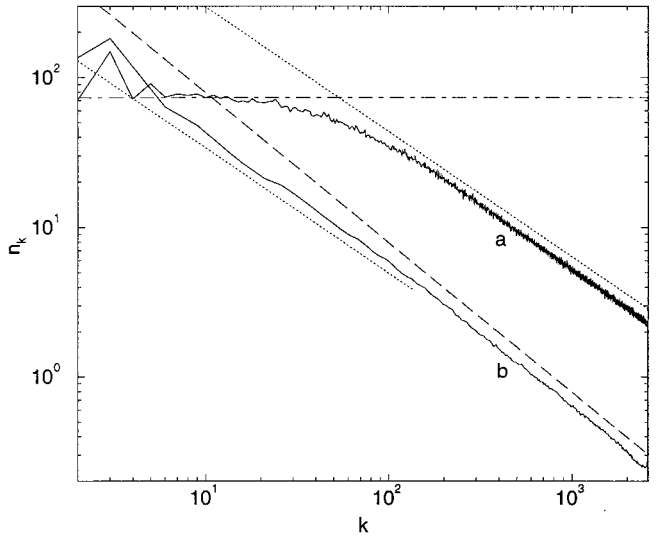

Fig. 7. (*a*) Coexistence of thermodynamical equilibrium and the *inverse* WT cascade, for the *focusing* nonlinearity ($\alpha = 1/2$, $\sigma = 0$), driven by a steady force on $|k| = 1$. The flat part of the spectrum (dot-dashed line) shows thermodynamical equilibrium. (*b*) Coexistence of the *inverse* and *direct* WT cascades. The dotted (dashed) line has the exponent of inverse (direct) WT cascade.

Nonlocality. Finally, we address the locality of resonant energy transfer in k-space, a property that underlies many prevalent intuitions about the energy transfer mechanisms of turbulence. Fig. 8 shows a case in which a WT direct cascade spectrum is observed for an intermediate k range. The system is forced at $|k| = 1$ only, while the broad range $2 \leq |k| \leq 10$ is strongly damped. The system reaches an SSS eventually, whose spectrum is depicted in Fig. 8. Strikingly, in this state, the power in the range $10 < |k| < 2600$ does not decay and is sustained by the $|k| = 1$ forcing alone, despite the little power and large dissipation in the range $1 < |k| \leq 10$. In light of this broad "blocking" dissipation, one may conclude that the flux in k space is highly *nonlocal*, although our system satisfies the locality requirement as defined in the usual sense of WT theories (2). This example illustrates that locality sometimes can be a subtle issue, at least for energy transfer from the pumping regime.

4. Conclusion

Taken together, these numerical experiments seem to indicate that, when there is a large "flow-rate" from the injection scales to the dissipation scales, the turbulent state is often described by the MMT spectrum—with fronts and leading edges in k-space profiles, and/or with growing norms. On the other hand, when there is relatively little "flow" from forcing to dissipation scales, the state is often described by WT—as in freely decaying turbulence with slowly decaying energy, and in steady states with constant mean energy. It also seems that the WT spectrum is an intrinsic property of the free wave system, whereas the MMT spectrum is associated with the entire driven-damped system. These indications are somewhat counter to the current intuition about dispersive wave turbulence, and certainly merit further investigation.

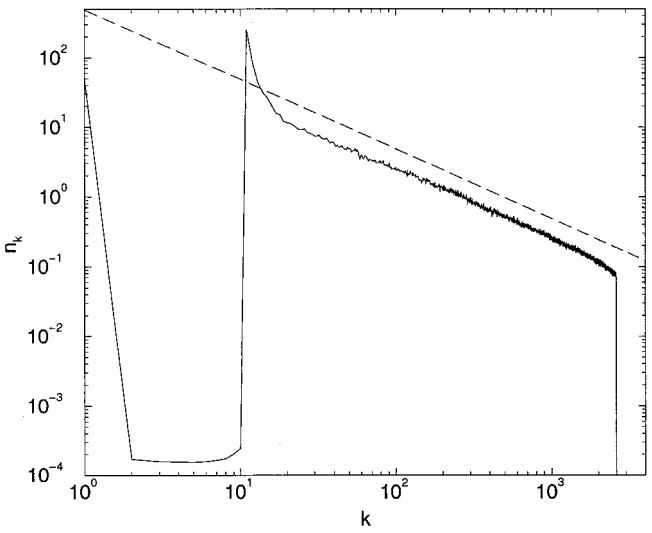

Fig. 8. Nonlocality. The WT direct cascade spectrum for focusing nonlinearity with $\alpha = 1/2$ and $\sigma = 0$ is sustained by forcing at $|k| = 1$, despite strong damping in $2 \leq |k| \leq 10$. The dashed line has the slope of WT direct cascade.

The following support is acknowledged: for D.C., Sloan Foundation #96-3-1; for A.M., National Science Foundation (NSF) DMS 9972865, DMS 9625795, ONR N00014-96-1-0043, and ARO-DAAG55-98-1-0129; for D.M., Sloan Foundation #96-3-1, AFOSR-49620-98, and NSF DMS 9971813; and for E.T., Alfred P. Sloan Fellowship and NSF DMS 9701751.

1. Majda, A. J., McLaughlin, D. W. & Tabak, E. G. (1997) *J. Nonlinear Sci.* **6,** 9–44.
2. Zakharov, V. E. (1984) *Handbook Plasma Phys.* **2,** 1–36.
3. Smith, L. & Yakhot, V. (1993) *Phys. Rev. Lett.* **71,** 352–355.
4. Smith, L. & Yakhot, V. (1994) *J. Fluid Mech.* **274,** 115–138.
5. Borue, V. (1993) *Phys. Rev. Lett.* **72,** 1475–1478.
6. Maltrud, M. & Vallis, G. (1991) *J. Fluid Mech.* **228,** 321–342.
7. Cai, D., McLaughlin, D. W. & Shatah, J. (1999) *Phys. Lett. A* **253,** 280–286.
8. Jordan, R., Turkington, B. & Zirbel, C., *Physica D.*, in press.
9. Falkovich, G. E. & Shafarenko, A. V. (1988) *Sov. Phys. JETP* **68,** 1393–1397.
10. Zakharov, V. E. (1984) *Handbook Plasma Phys.* **2,** 81–121.
11. Newell, A. C., Rand, D. A. & Russell, D. (1988) *Phys. Lett. A* **132,** 112–123.